Crown-containing butadienyl dyes
5.* Structure and photoisomerization of a butadienyl dye containing a 15-crown-5 fragment**

E. N. Ushakov,[a] S. P. Gromov,[b] L. G. Kuz´mina,[c] A. I. Vedernikov,[b] V. G. Avakyan,[b] J. A. K. Howard,[d] and M. V. Alfimov[b]*

[a]*Institute of Problems of Chemical Physics, Russian Academy of Sciences, 142432 Chernogolovka, Moscow Region, Russian Federation. Fax: +7 (096) 515 5420. E-mail: eushakov@icp.ac.ru*
[b]*Photochemistry Center, Russian Academy of Sciences, 7A ul. Novatorov, 119421 Moscow, Russian Federation.*
[c]*N. S. Kurnakov Institute of General and Inorganic Chemistry of Russian Academy of Sciences, 31 Leninsky prosp., 117907 Moscow, Russian Federation.*
[d]*Department of Chemistry, University of Durham, South Road, Durham DH1 3LE, UK*

The structure of the *E*,*E* isomer of a butadienyl dye of the benzothiazole series containing a 15-crown-5 fragment was established by X-ray diffraction analysis. The stacking motif of the dye molecules in the crystal structure is, apparently, attributable to intermolecular π-interactions between the large conjugated fragments. The possibility of [2+2] photocycloaddition occurring in the crystal is discussed. Reversible geometrical photoisomerization of the dye and its complex with Mg^{2+} in acetonitrile solution was studied by spectrophotometry and ^1H NMR spectroscopy. Photoirradiation of the complex of the *E*,*E* isomer with Mg^{2+} leads predominantly to isomerization of the C=C bond adjacent to the benzothiazole fragment. Regioselective *E*,*E*→*Z*,*E* photoisomerization occurs *via* a singlet mechanism with a quantum yield of about 0.45. The quantum yield of reverse *Z*,*E*→*E*,*E* photoisomerization is approximately 0.52. The structures of different geometrical isomers of the dye complex with Mg^{2+} were calculated by the quantum-chemical density functional theory (DFT).

Key words: crown ethers, butadienyl dyes, structure, complex formation, photoisomerization.

Extensive literature on chromogenic compounds, which contain a crown fragment conjugated with a chromophore and, hence, are capable of binding metal and ammonium cations, has been published in recent years. Particular attention has been given to crown-containing photochromic compounds, which can undergo substantial structural changes with the resulting change in the ability to bind cations upon exposure to light.[2,3] In this respect, crown-containing unsaturated compounds, primarily, styryl dyes,[4,5] show considerable promise. Upon photoirradiation, these compounds can undergo reversible geometrical isomerization at the ethylene C=C bond. This reaction can lead to a change in the stability constant of the dye complex with a metal ion by several orders of magnitude. Cation-dependent reversible [2+2] photocycloaddition resulting in the stereoselective formation of cyclobutane derivatives provides another example of photoreactions proceeding in dilute solutions of dimeric complexes of styryl dyes.

The introduction of one more C=C bond into the molecules of styryl dyes gives rise to the so-called butadienyl dyes.[6] The presence of the butadiene fragment instead of the ethylene group improves the optical characteristics of the compounds, due to which they can be used, for example, as laser dyes.[7] One would expect that butadienyl dyes will be involved in a broader spectrum of photoreactions compared to styryl analogs. Recently,[8] we have described the synthesis of new butadienyl dyes (*E*,*E*)-**1a—c** of the benzothiazole series with different sizes of crown fragments containg oxygen atoms conjugated with the chromophoric moiety of the molecules. Spectroscopic studies of the complex formation of (*E*,*E*)-**1a—c** with alkali and alkaline-earth metal ions demonstrated that crown-containing butadienyl dyes form more stable metal complexes and provide better color contrast upon binding of metal ions compared to the corresponding styryl

* For Part 4, see Ref. 1.

** Materials were presented at the Russian-French Symposium "Supramolecular Systems in Chemistry and Biology" (Kazan, September 22—25, 2003).

Published in Russian in *Izvestiya Akademii Nauk. Seriya Khimicheskaya,* No. 7, pp. 1491—1503, July, 2004.

1066-5285/04/5307-1549

analogs. Compound **1b** forms 2 : 1 complexes with the Sr^{2+} and Ba^{2+} ions. In these complexes, the planar chromophoric fragments are arranged in a head-to-head fashion due to stacking of two dye molecules, and the metal cation is bound to two crown fragments to form a sandwich complex.

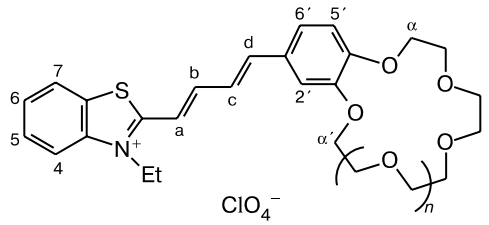

syn-(*E*,*E*)-**1a—c**

n = 0 (**a**), 1 (**b**), 2 (**c**)

The aim of the present study was to perform in-depth investigation of the structure and physicochemical properties of dye **1b**. The structure and molecular packing of this dye in the crystal are discussed. Quantum-chemical calculations were carried out for different geometrical isomers of the complex of **1b** with Mg^{2+}. Reversible *E*-*Z* photoisomerization of this complex in acetonitrile solution was studied experimentally.

X-ray diffraction study

The structures of the components of the crystal structure and the notations of the atoms in (*E*,*E*)-**1b** are given in Fig. 1. The crystal consist of the organic cations of the dye, the perchlorate anions, and the benzene solvate molecules in a ratio of 1 : 1 : 1 (selected bond lengths and bond angles in the cation are given in Table 1). The organic cation is virtually planar. The dihedral angles between the plane of the butadiene system and the planes of the benzothiazolium and benzene (C(9)...C(14)) fragments are 4.1 and 4.4°, respectively. Alternation of the bonds in the butadiene system C(12)—C(15)=C(16)—C(17)=C(18)—C(19) corresponds to formal localization of the single and double bonds (1.460(2), 1.352(2), 1.428(2), 1.359(2), and 1.430(2) Å, respectively). However, the double bonds are somewhat elongated, whereas the single bonds are shortened com-

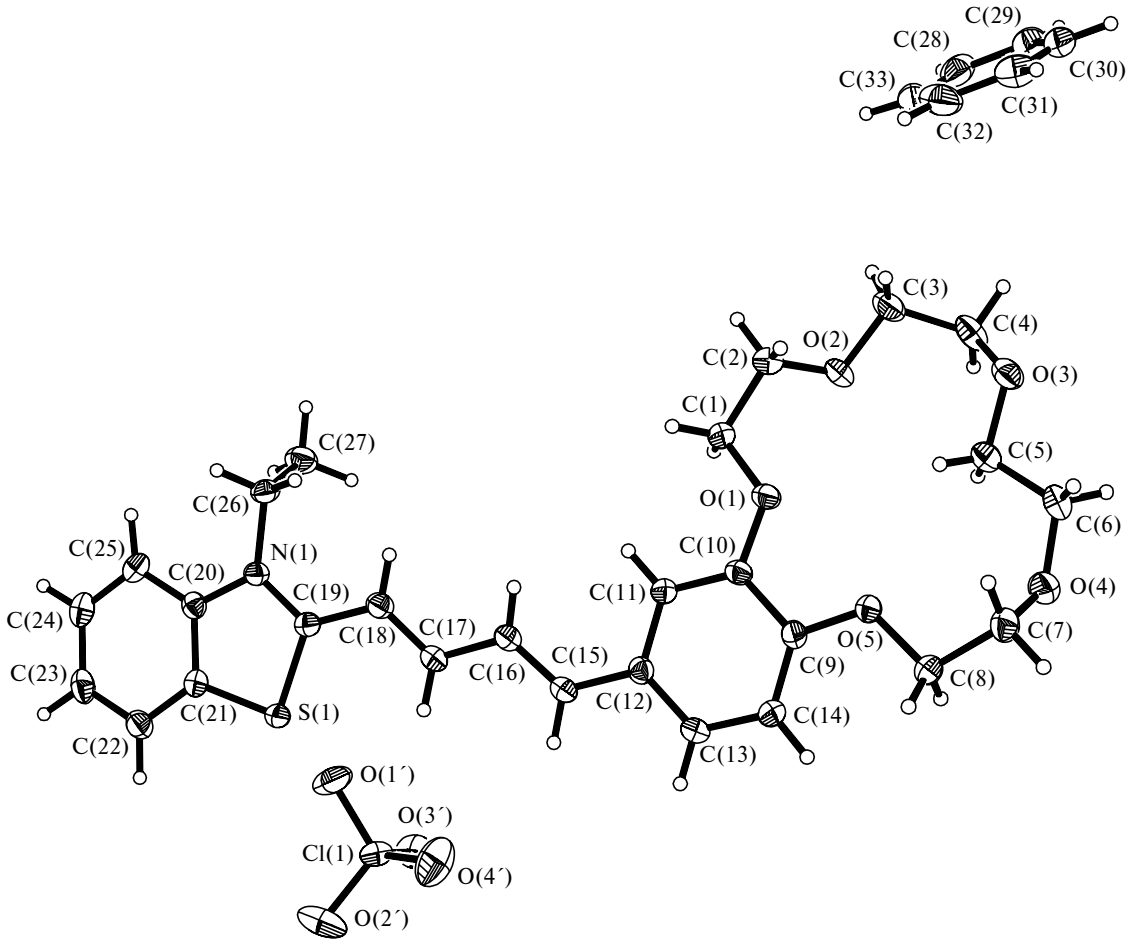

Fig. 1. Molecular structure of dye **1b** and the benzene solvate molecule.

Table 1. Selected bond lengths (*d*) and bond angles (ω) in the cation of **1b**

Bond	*d*/Å	Bond	*d*/Å	Angle	ω/deg
S(1)—C(19)	1.727(2)	N(1)—C(26)	1.484(2)	C(19)—S(1)—C(21)	91.18(8)
S(1)—C(21)	1.743(2)	C(9)—C(14)	1.383(2)	C(10)—O(1)—C(1)	116.9(1)
O(1)—C(10)	1.366(2)	C(9)—C(10)	1.419(2)	C(9)—O(5)—C(8)	117.8(1)
O(1)—C(1)	1.432(2)	C(10)—C(11)	1.381(2)	O(5)—C(9)—C(14)	125.5(1)
O(2)—C(2)	1.413(2)	C(11)—C(12)	1.413(2)	O(5)—C(9)—C(10)	114.7(1)
O(2)—C(3)	1.420(2)	C(12)—C(13)	1.396(2)	C(14)—C(9)—C(10)	119.8(1)
O(3)—C(4)	1.426(2)	C(12)—C(15)	1.460(2)	O(1)—C(10)—C(11)	124.8(1)
O(3)—C(5)	1.439(2)	C(13)—C(14)	1.399(2)	O(1)—C(10)—C(9)	115.38(14)
O(4)—C(7)	1.421(2)	C(15)—C(16)	1.352(2)	C(11)—C(10)—C(9)	119.81(14)
O(4)—C(6)	1.431(2)	C(16)—C(17)	1.428(2)	C(16)—C(15)—C(12)	125.10(16)
O(5)—C(9)	1.365(2)	C(17)—C(18)	1.359(2)	C(15)—C(16)—C(17)	123.96(16)
O(5)—C(8)	1.436(2)	C(18)—C(19)	1.430(2)	C(18)—C(17)—C(16)	121.86(16)
N(1)—C(19)	1.346(2)	C(20)—C(21)	1.399(2)	C(17)—C(18)—C(19)	123.26(16)
N(1)—C(20)	1.402(2)				

pared to the standard values (1.33 and 1.48 Å), which is indicative of the occurence of conjugation in the butadiene fragment of the dye.

The benzocrown fragment of **1b** shows characteristic features.[8—13] In the macrocyclic system, the exocyclic bond angles at the C(9) and C(10) atoms, *viz*., O(1)—C(10)—C(9) and O(5)—C(9)—C(10), are smaller (115.4 and 114.7°, respectively), whereas the endocyclic bond angles at the same atoms, *viz*., O(1)—C(10)—C(11) and O(5)—C(9)—C(14), are larger (124.8 and 125.5°, respectively) than the standard values. The distance between the O(1) and O(5) atoms (2.575 Å) is smaller than twice the van der Waals radius. This type of geometric distortions is opposite to that, which would be observed in the case of steric repulsion between the oxygen atoms. Apparently, this fact is attributable to conjugation of the lone electron pairs (LEP) of these oxygen atoms with the benzene ring. The geometry of the bonds involving these oxygen atoms is favorable for conjugation of the lone electron pair, which occupies the *p* orbital, with the π system of the benzene ring. Actually, the bond angles at the O(1) and O(5) atoms (116.9(1) and 117.8(1)°, respectively) correspond to their sp^2-hybridized state, and the $C_{Alk}—O—C_{Ar}—C_{Ar}$ torsion angles (−17.0 and −14.5°) are sufficiently small to provide the almost parallel arrangement of these orbitals. Earlier, we have observed an analogous type of distortions of the benzocrown fragment in related structures.[8,10—13] In one-half of the benzene ring, C(9)—C(10)—C(11)—C(12), the double bond is partially localized (1.419(2), 1.381(2), and 1.413(2) Å), whereas this effect is virtually absent in another half of the benzene ring involving the C(9)—C(14)—C(13)—C(12) atoms (1.383(2), 1.399(2), and 1.396(2) Å, respectively). The geometric parameters of the benzothiazolium fragment have standard values.[14]

It is of considerable interest to analyze the crystal packing of dye **1b** because it can allow conclusions to be drawn as to whether this dye can be subjected to [2+2] photocycloaddition an also about the structure of the resulting cyclobutane derivative. The crystal packing is shown in Fig. 2. The cations are packed in stacks. The side view of the structure of one stack is shown in Fig. 3.

The stacks are extended along the *a* axis. The pairs of the molecules are related by centers of symmetry, which belong alternately to two systems (*x*0*y* and *x*0.5*y*). The molecules of the A, B, and C types (the atomic numbering scheme includes the symbols A, B, and C) are related to each other by a translation along the *a* axis. The same is true for the molecules of the D and E types. Therefore, two types of superposition of the conjugated systems of molecules **1b** in the centrosymmetrical pairs ("dimers") alternate in the stacks (see Fig. 4).

One type of superposition (see Fig. 4, *a*) is characterized by a large distance between the nitrogen atoms on which the positive charges are formally localized (N(1A)...N(1D), 8.42 Å). Therefore, the Coulomb repulsion between the like charges is minimum. The distance between the planes of the butadiene fragments of the A and D molecules (3.52 Å) is typical of stacking interactions between aromatic or conjugated organic systems. In this pair of the cations, the butadiene fragments of the adjacent molecules are located in close proximity. The rather short C(15A)...C(18D) and C(16A)...C(17D) distances (3.78 and 3.85 Å, respectively) and the parallel arrangement of the C(15A)=C(16A) and C(18D)=C(17D) double bonds as well as the parallel arrangement of the C(15D)=C(16D) and C(18A)=C(17A) bonds are favorable for photocycloaddition in each of these pairs of the double bonds, but not in both of them simultaneously. Since two symmetrically related pairs of the closely spaced double bonds are in the absolutely identical crystal environment, the photochemical cycloaddition is unlikely to occur in the crystals characterized by this mutual arrangement of the cations of the dye. This

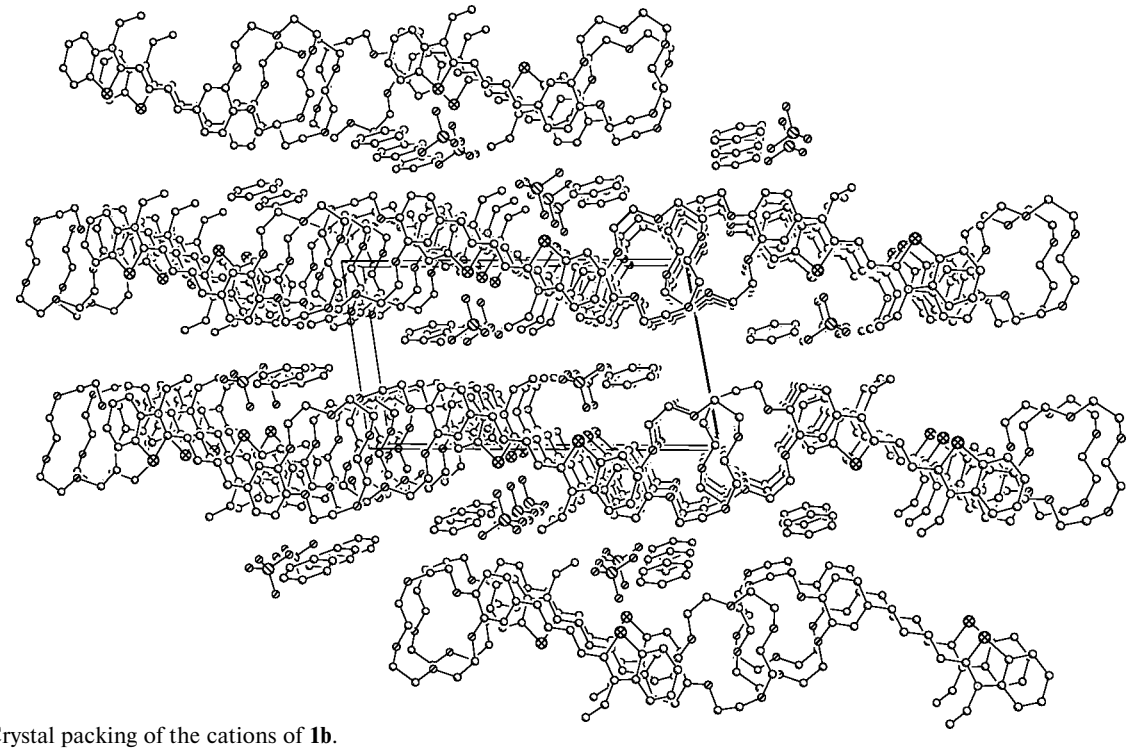

Fig. 2. Crystal packing of the cations of **1b**.

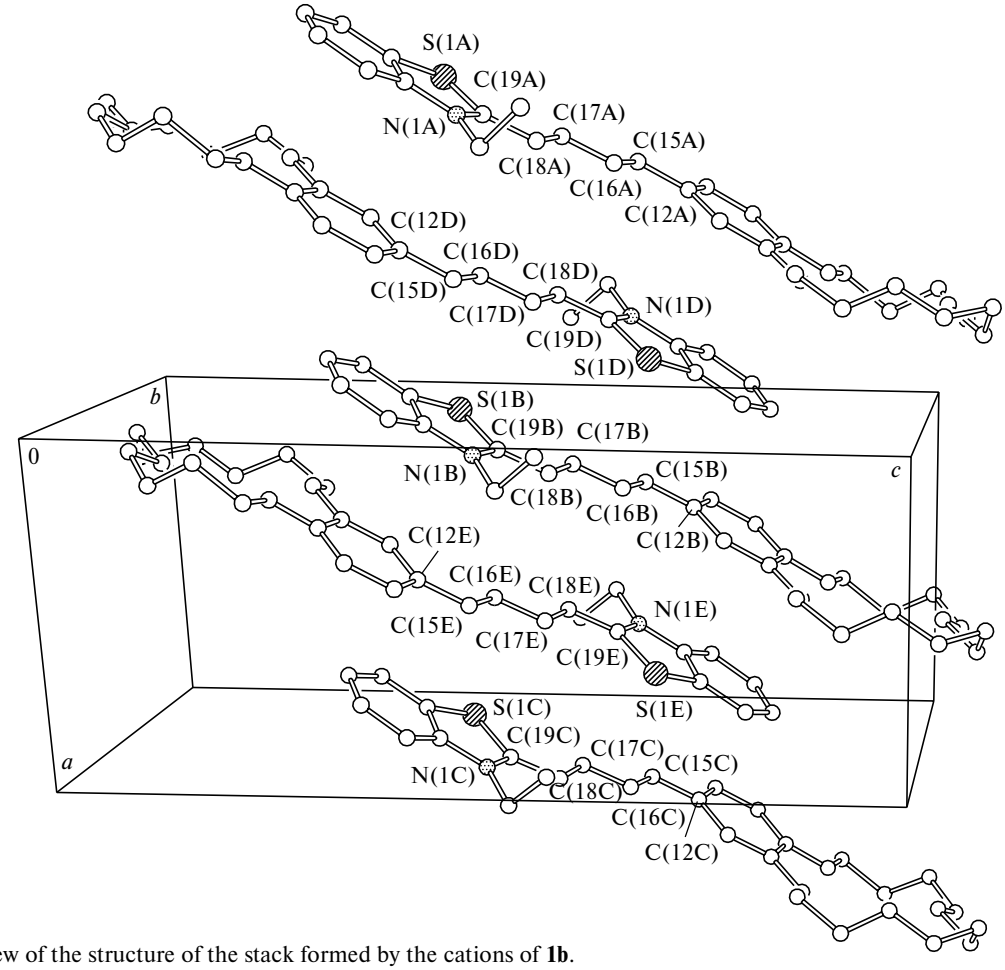

Fig. 3. Side view of the structure of the stack formed by the cations of **1b**.

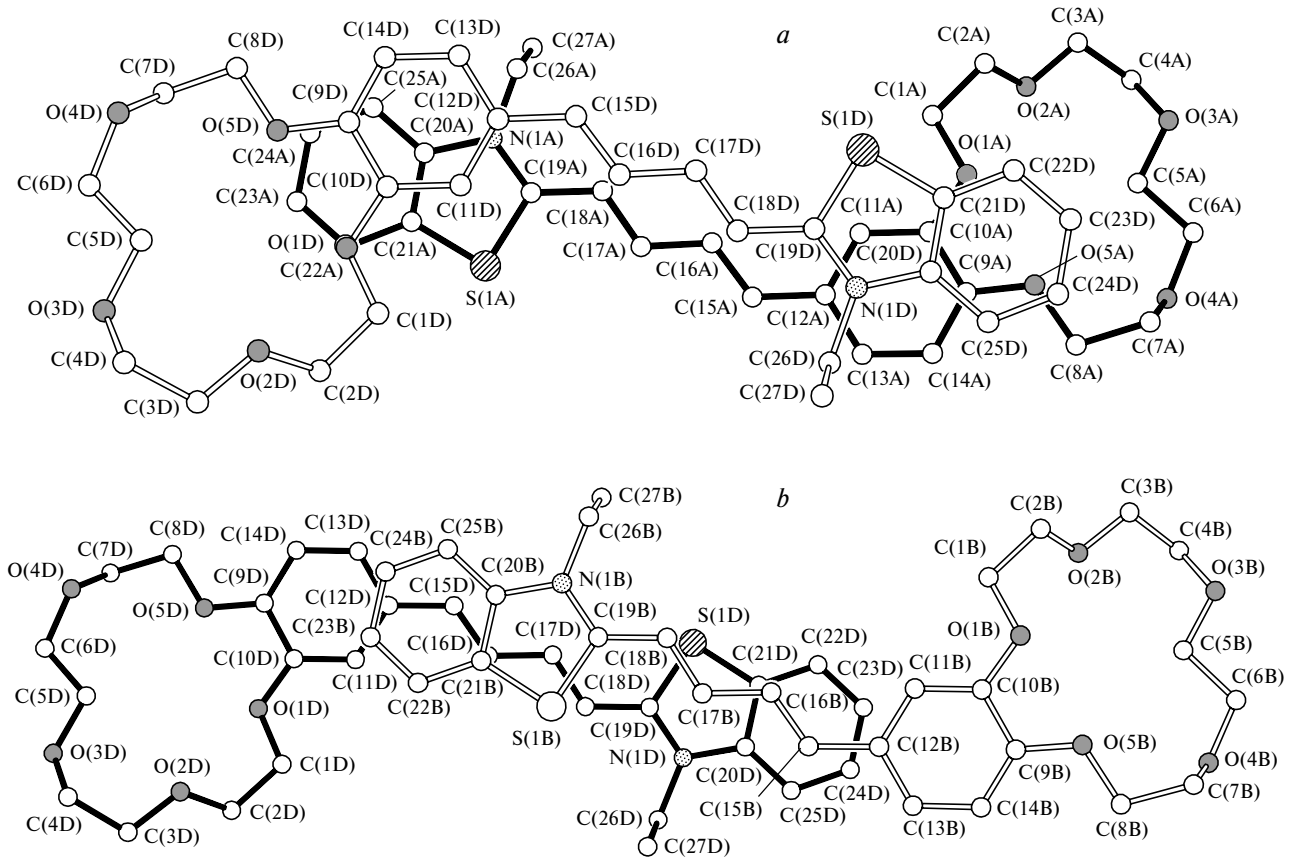

Fig. 4. Superposition of the pairs of the cations of **1b** related by different centers of symmetry on the mean plane of the butadiene system of one of the molecules in the pair.

reaction can proceed, if at all, only in an imperfect crystal lattice.

In the case of another type of superposition (see Fig. 4, *b*), the distance between the nitrogen atoms of the adjacent molecules is substantially shorter. The N(1B)...N(1D) distance (5.83 Å) is shorter than the analogous distance in the "upper" pair, and the distance between the planes of the butadiene fragments of the molecules in this pair increases to 3.72 Å. This increase in the distance is, apparently, attributable to Coulomb repulsions between the likely charged molecular systems. At the same time, the measured distance is also typical of stacking interactions. In this pair of the molecules, the benzothiazolium fragment is projected onto the butadiene system. The double bonds in the butadiene fragments are shifted with respect to each other in parallel planes. This mutual arrangement of the molecules in the pair results in an increase in the C(17B)...C(18D) and C(17D)...C(18B) distances to 4.48 Å, and the double bonds are parallel to each other. This geometry does not exclude the possibility of photochemical [2+2] cycloaddition. However, the increasing Coulomb repulsion prevents these double bonds from approaching each other in the course of photocycloaddition, because this process should be accompanied by a decrease in the distance between the positively charged thiazolium fragments of two molecular cations. This situation is highly improbable in the solid phase because it would require substantial shifts of the atoms of the adjacent molecules toward each other.

The third type of the mutual arrangement of the butadiene systems resulting in a close arrangement of the bonds of the C(15)=C(16) type in two parallel molecule does not occur in the crystal, although it is this arrangement that will lead to the maximum distance between the charged benzothiazolium fragments. Apparently, the occurrence of this dimeric structure in the crystal is in contradiction with the the earlier-mentioned fact[8–12] that all crown-ether dyes tend to form hydrophilic regions (channels and layers) composed of the crown fragments.

In the crystal structure, the crown fragments are alternately located on opposite sides of the stack formed by the cations. The superposition of the stacks along the *c* axis gives rise to a layer, in which the crown fragments of each stack "penetrate" into the adjacent stacks to form a crown-ether channel parallel to the stacks, *i.e.*, along the *b* axis (Fig. 5).

In the crystal, both the perchlorate anions and the benzene solvate molecules are located between the layers

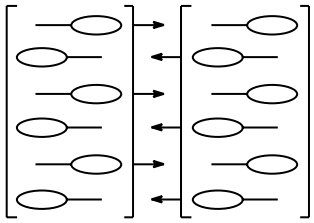

Fig. 5. Orientation of the crown fragments and the formation of the crown-ether channel.

(see Fig. 2). The planes of the benzene solvate molecules are almost perpendicular to the mean planes of the cations. Interestingly, the crown-ether channels of the adjacent layers in the crystal are located in the vicinity of each other. This gives rise to bulky hydrophilic layers characterized by a very loose packing stabilized due to filling of the crystal space by benzene molecules. In the crystal, no significant weak interactions involving the oxygen atoms of the anions are observed.

Spectroscopic study of geometrical photoisomerization

Earlier, we have measured the ^{1}H NMR, UV-Vis absorption, and luminescence spectra for the *E*,*E* isomer of dye **1b** and its complex with Mg^{2+}.[8] In the present study, we investigated the kinetics and regioselectivity of reversible *E*-*Z* photoisomerization of the dye and its complex with Mg^{2+} by spectroscopic methods.

Irradiation of (*E*,*E*)-**1b** in acetonitrile with visible light led to a decrease in the intensity and a small hypsochromic shift of the long-wavelength band in the UV-Vis absorption spectrum of the dye as well as to an increase in the intensity of absorption associated with higher-energy electron transitions. These spectral changes are typical of geometrical isomerization of butadienes containing electron-releasing and -withdrawing groups at positions 1 and 4, respectively.[15] Dye **1b** belongs to this class of compounds. Unlike 1,2-disubstituted ethylenes for which only one *Z* photoisomer can occur, asymmetrical 1,4-disubstituted butadienes can exist as three *Z* photoisomers, *viz.*, *E*,*Z*, *Z*,*E*, and *Z*,*Z*. The latter isomer is generally formed in very small amounts, because in the excited state the *E*,*Z*→*Z*,*Z* and *Z*,*E*→*Z*,*Z* reactions proceed more slowly than the corresponding reverse reactions, *i.e.*, *E*,*Z*→*E*,*E* and *Z*,*E*→*E*,*E*. The ratio between the *E*,*Z* and *Z*,*E* photoisomers varies within a broad range depending on the nature of the substituents.[16]

Upon storage of an irradiated solution of the dye in the dark, the spectrum of the *E*,*E* isomer is restored to its original form due to reverse dark (thermal) isomerization of the *Z* photoisomers. Hence, we failed to study the structures of the photoisomers and obtain accurate quantitative data on the kinetics of photoisomerization.

It should be noted that reverse dark isomerization of the *Z* photoisomers of **1b** is readily catalyzed by trace amounts of impurities characteristic of acetonitrile. Earlier, we have observed catalytic *Z*→*E* isomerization of styryl analogs of dye **1b**. However, the mechanism of this phenomenon has not been studied in detail. Presumably, the mechanism involves the reversible addition of an impurity base to the ethylene C=C bond of the dye. We know from experience that impurities, which catalyze dark *Z*→*E* isomerization of styryl dyes, may be present even in acetonitrile of special purity grade. In addition, samples of dyes may also contain trace amounts of catalytic impurities depending on the procedure for their preparation. Hence, we do not publish the observed rate constant of dark *Z*→*E* isomerization for **1b**, because it may differ substantially from the true rate constant of thermal isomerization.

The absorption spectrum of the complex of (*E*,*E*)-**1b** with Mg^{2+} in acetonitrile solution and the spectra of the photostationary states established upon prolonged irradiation of the complex at a wavelength of 313, 365, 405, or 436 nm are shown in Fig. 6. This figure also presents the dependence of the absorption spectrum of the complex on the time of its stationary irradiation at λ = 365 nm. The absorption spectra underwent no changes upon storage of irradiated solutions of the complex in the dark for

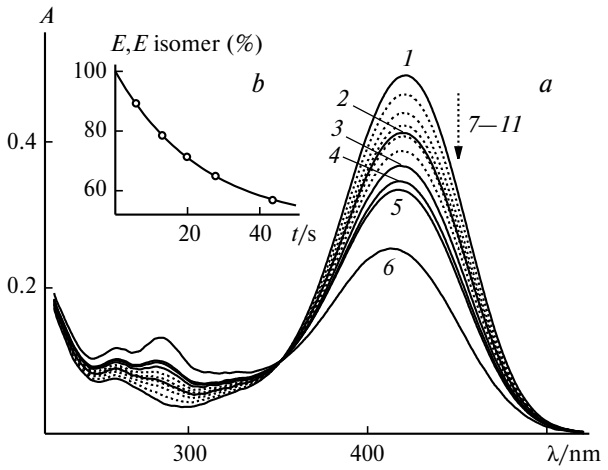

Fig. 6. *a*, Influence of photoirradiation on the absorption spectrum of the complex of **1b** with Mg^{2+} in acetonitrile (1-cm cell, the complex was prepared by the addition of magnesium perchlorate to a solution of **1b** ($1.0 \cdot 10^{-5}$ mol L^{-1}) to the concentration of $1.0 \cdot 10^{-3}$ mol L^{-1}): *1*, the spectrum of [(*E*,*E*)-**1b**]·Mg^{2+}; *2*—*5*, the spectra of photostationary states established upon irradiation of the complex at a wavelength of 313 (*2*), 365 (*3*), 405 (*4*), or 436 nm (*5*); *6*, the calculated spectrum of [(*Z*,*E*)-**1b**]·Mg^{2+}; *7*—*11*, the spectra measured after irradiation of [(*E*,*E*)-**1b**]·Mg^{2+} at λ = 365 nm with an intensity of $1.5 \cdot 10^{-6}$ Einstein L^{-1} s^{-1} for 5.7 (*7*), 13.0 (*8*), 19.8 (*9*), 27.7 (*10*), and 43.5 s (*11*); *b*, the dependence of the percentage content of the *E*,*E* photoisomer on the irradiation time (the solid line corresponds to the kinetics of the reversible first-order reaction).

at least one day. The general pattern of photoinduced spectral changes and the existence of photostationary states, which have different absorption spectra, provide evidence that the complex of **1b** with Mg^{2+} undergoes reversible *E*-*Z* photoisomerization. Relatively high thermal stability of the *Z* photoisomers of the dye complex with Mg^{2+} can be interpreted in terms of disruption of conjugation in the butadiene chain due to the electron-withdrawing effect of the coordinated metal ion (see the results of quantum-chemical calculations described below). In addition, when studying model styryl and butadienyl dyes of the benzothiazole series, which contain two methoxy groups instead of the crown fragment, we found that magnesium perchlorate can neutralize the effect of impurities, which catalyze reverse dark $Z \rightarrow E$ isomerization.

To estimate the number of *Z* photoisomers of the dye that formed, the complete set of experimental spectra presented in Fig. 6, *a* was analyzed using the singular value decomposition (SVD). It was found that 99.5% of the total spectral variation is described by two principal SVD vectors, *i.e.*, the reaction system under consideration behaves (in the first approximation) as a two-component system. However, we cannot completely exclude the possibility that the system contains a small fraction of other components, because two principal SVD vectors generally describe $\geq$99.9% of the total spectral variation in the case of true two-component systems.

When determining the quantum yields of the reversible *E*-*Z* photoisomerization of the complex of **1b** with Mg^{2+}, we assumed that, first, only one of three possible *Z* photoisomers is formed and, second, the ratio of the quantum yields of the forward and reverse photoisomerization is independent of the irradiation wavelength. Under these constraints, the absorption spectrum of the *Z* photoisomer can be easily calculated if the spectrum of the *E* isomer and the spectra of at least two different photostationary states are known. In the case of the complex of **1b** with Mg^{2+}, the spectrum of the *Z* photoisomer was determined using the simple yet very efficient self-modeling method as applied to the spectral matrix (see the Experimental section). The spectral matrix included the absorption spectrum of $[(E,E)\text{-}\mathbf{1b}] \cdot Mg^{2+}$ and the spectra measured for four different photostationary states. The calculated spectrum of the *Z* photoisomer is shown in Fig. 6. The percentage contents of both isomers in different stationary states are given in Table 2. This table lists also the quantum yields of the forward and reverse photoisomerization for the complex of **1b** with Mg^{2+}. The quantum yields were determined from the dependence of the percentage content of the *E*,*E* photoisomer on the time of irradiation at $\lambda = 365$ nm (see Fig. 6, *b*).

The high quantum yields of photoisomerization in a solution containing atmospheric oxygen indicate that the reaction proceeds *via* a singlet mechanism. The radiation lifetime of the excited singlet state S_1 for $[(E,E)\text{-}\mathbf{1b}] \cdot Mg^{2+}$, which was estimated from the integrated extinction coefficient of the long-wavelength absorption band, is about 3 ns. The time constant of radiationless deactivation for the S_1 state, which was calculated from the radiation lifetime and the known quantum yield of fluorescence of $[(E,E)\text{-}\mathbf{1b}] \cdot Mg^{2+}$ in acetonitrile (0.0016),[8] is approximately 5 ps. In the case of $[(E,E)\text{-}\mathbf{1b}] \cdot Mg^{2+}$, radiationless deactivation of the S_1 state occurs almost completely through isomerization. Hence, we, in fact, estimated the time constant of isomerization in the excited singlet state. The value of this constant is indicative of a very low barrier to isomerization in the excited state of $[(E,E)\text{-}\mathbf{1b}] \cdot Mg^{2+}$.

The photostationary state, which was established upon irradiation of the complex of **1b** with Mg^{2+} at $\lambda = 365$ nm, was studied by ^{1}H NMR spectroscopy. The preparation of the sample is described in the Experimental section. The NMR spectrum of the photostationary mixture is shown in Fig. 7. For comparison, Fig. 7 also presents the NMR spectra of the *E*,*E* isomer of **1b** and its complex with Mg^{2+} (the atomic numbering scheme is given in the formula **1**).

The spectrum of the photostationary mixture has two major sets of signals, one of which belongs to the complex of the *E*,*E* isomer, whereas another one corresponds to the complex of one of three theoretically possible *Z* photoisomers of the dye. Other relatively low-intensity signals belong, apparently, to the complexes of two other theoretically possible *Z* photoisomers. For a freshly prepared sample, the molar ratio between the *E*,*E* isomer

Table 2. Spectroscopic characteristics of the $[(E,E)\text{-}\mathbf{1b}] \cdot Mg^{2+}$ and $[(Z,E)\text{-}\mathbf{1b}] \cdot Mg^{2+}$ complexes, the percentage contents of the *E*,*E* and *Z*,*E* isomers in various photostationary states and the quantum yields of the forward and reverse photoisomerization[a]

Isomer	λ_{max} /nm	ε_{max} /mol^{-1} L^{-1} cm^{-1}	φ_{iso}	Content (%)			
				313 nm	365 nm	405 nm	436 nm
$[(E,E)\text{-}\mathbf{1b}] \cdot Mg^{2+}$	421	49200	0.45	67.6	48.5	39.4	35.1
$[(Z,E)\text{-}\mathbf{1b}] \cdot Mg^{2+}$	414	25400	0.52	32.4	51.5	60.6	64.9

[a] In MeCN in the presence of atmospheric oxygen.

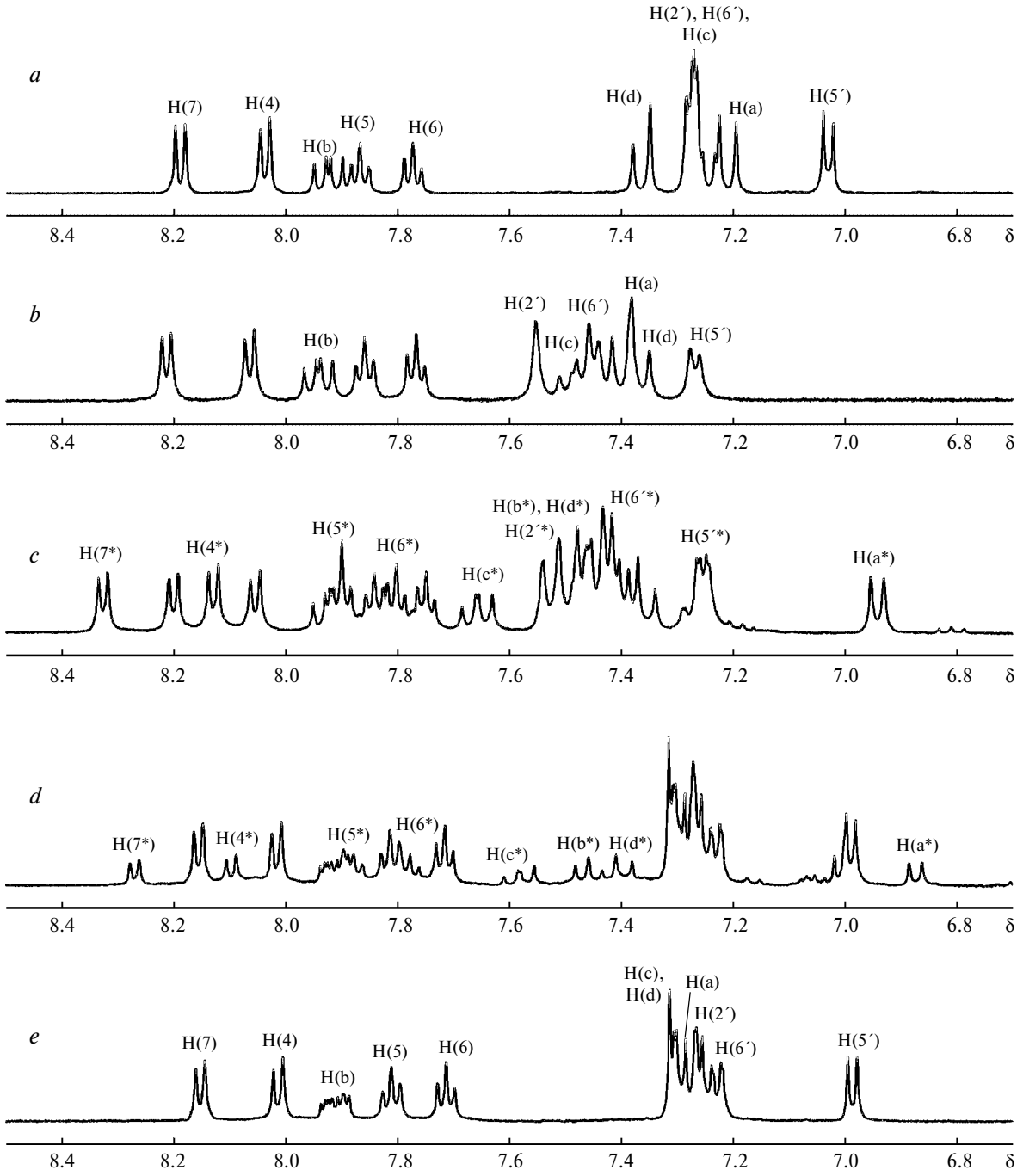

Fig. 7. ^{1}H NMR spectra of dye **1b** (~$5 \cdot 10^{-3}$ mol L^{-1}) in CD_3CN at 25 °C: *a*, (*E*,*E*)-**1b**; *b*, (*E*,*E*)-**1b** in the presence of $Mg(ClO_4)_2$ (0.1 mol L^{-1}); *c*, a photostationary mixture of the geometrical isomers of **1b** (see the Experimental section) in the presence of $Mg(ClO_4)_2$ (0.1 mol L^{-1}); *d*, the same sample after the addition of D_2O (10%, by volume); *e*, the same sample after 30 min.

and the major *Z* photoisomer, which was estimated from the integral intensity of the signals for the protons of the same type, is 48 : 52. This value is consistent with the data from UV-Vis absorption spectroscopy.

The addition of D_2O to a solution containing a mixture of geometrical isomers of the complex of **1b** with Mg^{2+} led to dissociation of the metal cation—macrocycle complex due to strong solvation of the Mg^{2+} ions with water molecules. The signals of the free major *Z* photoisomer, which were observed in the NMR spectrum immediately after the addition of water (Fig. 7, *d*), completely disappeared within < 30 min (Fig. 7, *e*) due to relatively fast dark isomerization giving rise to the *E*,*E* isomer. The weak signals of the minor photoproducts

Scheme 1

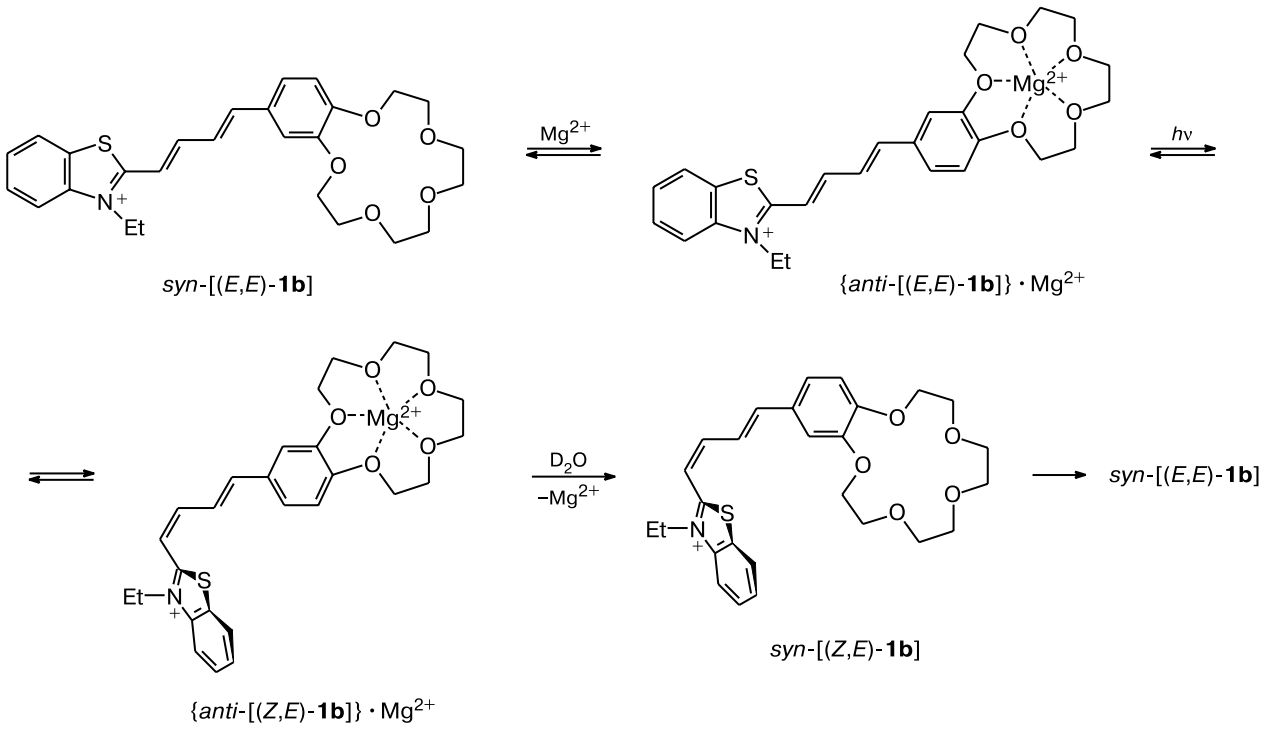

also completely disappeared after the addition of water, which indicates that these signals belong to two other theoretically possible *Z* photoisomers.

The structure of the major *Z* photoisomer was established based on the 2D COSY and NOESY spectra measured for a sample of the complex of **1b** with Mg^{2+} irradiated at $\lambda = 365$ nm. The assignment of the signals for the protons is shown in Fig. 7, *c* (the signals of the *Z* photoisomer are marked with an asterisk in the atom numbers). Since the characteristic signal of the *Z* photoisomer at δ 6.94 appears as a doublet with the spin-spin coupling constant of 11.5 Hz, it can be assigned to one of the two protons at the *cis*-C=C bond of the butadiene fragment. In the NOESY spectrum, this proton gives an intense cross-signal with the protons of the CH_2N group (Fig. 8) and, hence, it is assigned to the H(a*) proton. The signal for the H(c*) proton at the *trans*-C=C bond appears as an individual doublet of doublets with the spin-spin coupling constants $J_{H(c^*),H(d^*)} = 14.6$ Hz and $J_{H(c^*),H(b^*)} = 12.4$ Hz, which is indicative of its transoid *s* conformation with respect to the H(b*) proton. In spite of the fact that all other signals for the butadiene protons of the *Z* photoisomer overlap with the signals for the protons of the *E,E* isomer, their positions are easily determined from the cross-signals with the H(a*) and H(c*) protons present in the COSY spectrum. Therefore, we can state with assurance that the major *Z* photoisomer found in the photostationary mixture has the *Z,E* configuration, *i.e.*, photoisomerization of the complex of **1b** with Mg^{2+} occurs predominantly at the C=C double bond adjacent to the benzothiazolium fragment (Scheme 1).

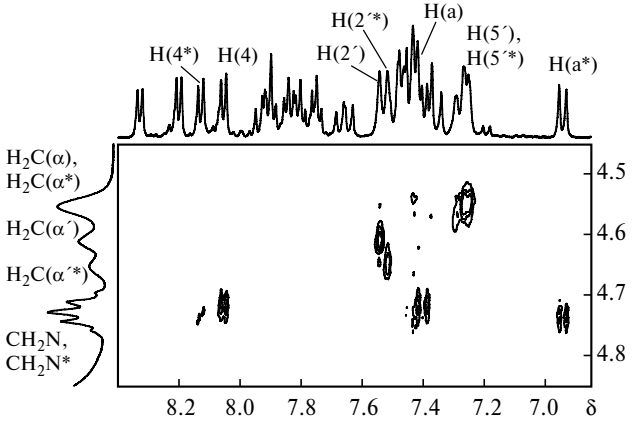

Fig. 8. The NOESY spectrum of a mixture of the *E,E* and *Z,E* isomers of dye **1b** (~$5 \cdot 10^{-3}$ mol L^{-1}) in CD_3CN in the presence of $Mg(ClO_4)_2$ (0.1 mol L^{-1}) at 25 °C.

The ratio between the *anti* and *syn* conformers (*s* rotamers) for the complex of the *Z,E* isomer with Mg^{2+} cannot be determined by NMR spectroscopy because of the overlap of some signals. Most likely, the equilibrium between the *s* rotamers for the complex of the *Z,E* isomer, like that for the complex of the *E,E* isomer,[8] is shifted toward the *anti* conformer, in which the Coulomb inter-

action between the likely charged fragments of the complex is weaker for geometric reasons.

It should be noted that the signals for the H(a) and H(b) protons of the butadiene fragment are substantially shifted upfield in going from [(*E*,*E*)-**1b**]·Mg^{2+} to [(*Z*,*E*)-**1b**]·Mg^{2+} ($\Delta\delta_H$ = 0.46 and 0.45, respectively). Apparently, these shifts are associated with weakening of the electron-withdrawing effect of the benzothiazolium fragment because the π conjugation in the butadiene chain of the *Z*,*E* conformer is disrupted. The observed upfield shifts can also be partially attributable to the fact that the above-mentioned protons move from the region of deshielding to the region of shielding of the benzothiazole fragment as a result of twisting around the C(2)—C(a) bond caused by steric interactions. By contrast, the signals for all protons of the heterocyclic fragment are shifted downfield by 0.05—0.13 ppm in going from [(*E*,*E*)-**1b**]·Mg^{2+} to [(*Z*,*E*)-**1b**]·Mg^{2+}, which is evidently associated with a slight increase in the positive charge density on this fragment.

Irradiation of a solution of [(*E*,*E*)-**1b**]·Mg^{2+} in CD_3CN using an incandescent lamp (100 W) for 2 h directly in an NMR tube (the distance to the source was 30 cm) afforded an isomeric mixture containing the same major components as those present in the mixtures obtained in experiments with the use of monochromatic irradiation. The molar ratio between the *E*,*E* and *Z*,*E* isomers was 37 : 63.

Quantum-chemical calculations

Earlier,[8] the rotational isomerism about C—C single bonds (*s* isomerism) for the *E*,*E* isomer of dye **1b** and its complex with Mg^{2+} has been investigated by quantum-chemical methods. It has been demonstrated that the *syn* conformer is energetically most favorable for the free dye, whereas the *anti* conformer is energetically most favorable for the dye complex with Mg^{2+} (Fig. 9). In the present study, we carried out in-depth theoretical investigation of isomerism of dye **1b**.

The calculations were performed by the density functional theory (DFT). The carbon—carbon bond lengths, torsion angles, and conformational characteristics of the macroheterocycle of *syn*-[(*E*,*E*)-**1b**] predicted by this method (see Fig. 9) agree well with the results of X-ray diffraction analysis (see Fig. 1).

The butadiene fragment in molecule **1b** has five rotational degrees of freedom, which correspond to 32 rotational isomers that differ from each other in the dihedral angles. The numbering of the bonds (r_1—r_5) and dihedral angles (τ_1—τ_5) for the butadiene fragment of molecule **1b** is presented in Fig. 9. Initially, all isomeric structures

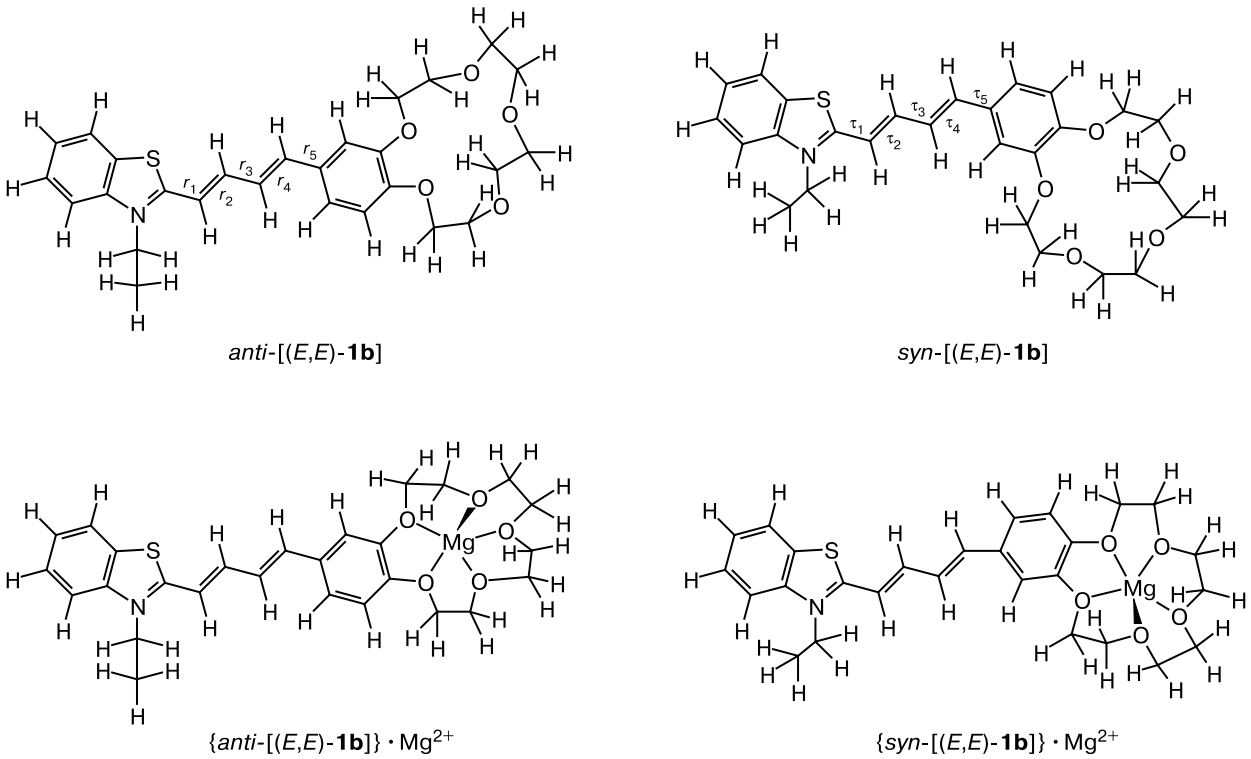

Fig. 9. Structures of the *anti* and *syn* conformers of the *E*,*E* isomer of **1b** and its complex with the magnesium cation calculated by the DFT method.

were fully optimized by the PM3 method. Each of 32 optimized structures is characterized by a set of $3N - 6$ ($N = 66$ atoms) positive harmonic vibrational frequencies, which is evidence that these structures correspond to local minima on the potential energy surface (PES). As expected, two structures, *viz.*, *anti*-[(*E*,*E*)-**1b**] and *syn*-[(*E*,*E*)-**1b**], correspond to the global minimum. The energy differences between these structures is only 0.16 kcal mol^{-1} in favor of the *syn* conformer, *i.e.*, the calculation predicted that under conditions of thermodynamic equlibrium, these *s* conformers should coexist in solution in comparable amounts. For both conformers, the dihedral angles τ_1—τ_5 are close to 0 or 180°. The DFT calculations for *anti*-[(*E*,*E*)-**1b**] and *syn*-[(*E*,*E*)-**1b**] with full geometry optimization also gave similar energies for these *s* conformers (Table 3). According to the results of calculations by the PM3 method, next in the energy (in order of increasing energy) are the pairs of the *anti* and *syn* conformers of the *Z*,*E* and *E*,*Z* isomers of **1b**.

The Mg^{2+} ion was introduced into the crown ring of all six isomeric structures. Then all structures of the complexes were calculated by the DFT method with full geometry optimization. The results of calculations are given in Tables 3 and 4. All calculated structures of the complexes have $3N - 6$ ($N = 67$ atoms) positive harmonic vibrational frequencies, which indicates that these structures correspond to local minima on the PES.

As in the case of the free dye, the *anti*-(*E*,*E*) and *syn*-(*E*,*E*) isomers of the complex are energetically most favorable, and the butadiene fragments are virtually planar. The complex formation leads to a decrease in the degree of delocalization of the π-electron density in the butadiene fragment. The formally double bonds in this fragment become shorter, whereas the formally single bonds become longer. The bond orders in this fragment change analogously, *i.e.*, the C=C bonds are strengthened and the C—C bonds are weakened. A decrease in the degree of conjugation in the butadiene fragment upon

Table 3. Total energies E_{total}, the zero-point energies (*ZPE*) in the harmonic approximation, the energies E_0[a] at 0 K, and the relative energies ΔE for different isomers of **1b** and their complexes with Mg^{2+} calculated by the DFT method

Isomer	$-E_{total}$	$-ZPE$	$-E_0$	ΔE_1[c]	ΔE_2[d]
	a.u. [b]			kcal mol^{-1}	
anti-[(*E*,*E*)-**1b**]	1875.514864	0.532380	1874.982484	—	0.0
syn-[(*E*,*E*)-**1b**]	1875.515615	0.532575	1874.983041	—	–0.3
{*anti*-[(*E*,*E*)-**1b**]}·Mg^{2+}	2074.949012	0.537234	2074.411778	0.0	0.0
{*syn*-[(*E*,*E*)-**1b**]}·Mg^{2+}	2074.945853	0.537225	2074.408627	2.0	2.0
{*anti*-[(*Z*,*E*)-**1b**]}·Mg^{2+}	2074.939592	0.537502	2074.402090	6.1	0.0
{*syn*-[(*Z*,*E*)-**1b**]}·Mg^{2+}	2074.933851	0.537599	2074.396253	9.7	3.6
{*anti*-[(*E*,*Z*)-**1b**]}·Mg^{2+}	2074.936349	0.537454	2074.398895	8.1	0.0
{*syn*-[(*E*,*Z*)-**1b**]}·Mg^{2+}	2074.928498	0.537313	2074.391185	12.9	4.8

[a] $E_0 = E_{total} + ZPE$.
[b] Atomic units.
[c] The energy of the complex relative to the most stable conformer: $\Delta E_1 = E_0$(complex) — — E_0({*anti*-[(*E*,*E*)-**1b**]}·Mg^{2+}).
[d] The energy of the *syn* conformer relative to the corresponding *anti* conformer: $\Delta E_2 = E_0$(*syn*) — — E_0(*anti*).

Table 4. Bond lengths (r/Å) and dihedral angles (τ/deg) in the butadiene fragment of different isomers of **1b** and their complexes with Mg^{2+} calculated by the DFT method

Structure	r_1	τ_1	r_2	τ_2	r_3	τ_3	r_4	τ_4	r_5	τ_5
anti-[(*E*,*E*)-**1b**]	1.409	177.7	1.386	179.7	1.407	179.7	1.382	179.9	1.430	179.7
syn-[(*E*,*E*)-**1b**]	1.409	178.7	1.386	180	1.407	179.7	1.382	179.8	1.429	1.8
{*anti*-[(*E*,*E*)-**1b**]}·Mg^{2+}	1.433	177.4	1.369	180	1.432	179.7	1.365	179.6	1.459	179.6
{*syn*-[(*E*,*E*)-**1b**]}·Mg^{2+}	1.434	179.6	1.368	180	1.433	178.8	1.365	179.6	1.457	4.8
{*anti*-[(*Z*,*E*)-**1b**]}·Mg^{2+}	1.433	169.3	1.372	4.6	1.435	178.4	1.366	178.2	1.458	179.5
{*syn*-[(*Z*,*E*)-**1b**]}·Mg^{2+}	1.432	170.1	1.371	5.9	1.437	175.4	1.366	178.4	1.458	11.5
{*anti*-[(*E*,*Z*)-**1b**]}·Mg^{2+}	1.432	177.8	1.370	177.9	1.435	179.0	1.368	6.6	1.462	161.1
{*syn*-[(*E*,*Z*)-**1b**]}·Mg^{2+}	1.431	176.6	1.370	175.0	1.436	175.4	1.364	8.3	1.468	40.7

the introduction of the magnesium cation into the coordination sphere of the crown fragment indicates that the metal cation in this system acts as an acceptor of the electron density. The coordination environment about the magnesium cation resembles a distorted tetragonal pyramid, the electron densities on all five Mg—O bonds being virtually equal (see Fig. 9).

Next in the energy (in order of increasing energy) after the pair of the *s* conformers of the complex [(*E*,*E*)-**1b**]·Mg^{2+} are the *anti* conformers of [(*Z*,*E*)-**1b**]·Mg^{2+} and [(*E*,*Z*)-**1b**]·Mg^{2+} and then the *syn* conformers of these complexes. The energy of the most stable *Z* isomer of the complex, *viz.*, {*anti*-[(*Z*,*E*)-**1b**]}·Mg^{2+}, is 6.1 kcal mol^{-1} higher than the energy of the most stable *E*,*E* isomer, *viz.*, {*anti*-[(*E*,*E*)-**1b**]}·Mg^{2+}. This provides evidence that the percentage of the *Z* isomers of the complex in the equilibrium in the absence of irradiation should be insignificantly small. The torsion angles τ_2 for the *cis*-(—C=C—) fragment in the *anti* and *syn* conformers of [(*Z*,*E*)-**1b**]·Mg^{2+} are 4.6 and 5.9°, respectively. The *anti* and *syn* conformers of [(*E*,*Z*)-**1b**]·Mg^{2+} are more nonplanar. In these conformers, the torsion angles τ_4 in the *cis*-(—C=C—) fragment are 6.6 and 8.3°, respectively. This pair is characterized by the maximum deviation of the plane of the substituent at the *cis*-C=C bond (in the case under consideration, of the benzene ring) from the plane of the butadiene fragment. Hence it follows that the steric factor is the main reason for the higher energies of the *s* conformers of [(*E*,*Z*)-**1b**]·Mg^{2+} compared to the corresponding *s* conformers of [(*Z*,*E*)-**1b**]·Mg^{2+}.

Earlier, it has been demonstrated[8] that the complex formation of (*E*,*E*)-**1b** with Mg^{2+} leads to the shift of the equilibrium between the *anti* and *syn* conformers toward the former one. According to the results of calculations by the Boltzmann equation, the complex formation leads to an increase in the equilibrium contribution of the *anti* conformer of (*E*,*E*)-**1b** at 25 °C from 37.6 to 96.7%. This effect is attributable to a weaker Coulomb interaction between the likely charged fragments of the complex in the more "extended" *anti* conformer. Apparently, the same effect is manifested in the case of the *Z* isomers of **1b**. For [(*Z*,*E*)-**1b**]·Mg^{2+} and [(*E*,*Z*)-**1b**]·Mg^{2+}, the calculated equilibrium contributions of the *anti* conformer are 99.8 and >99.9%, respectively.

To summarize, we carried out crystallographic study of the 15-crown-5-containing butadienyl dye of the benzothiazole series and analyzed the characteristic features of its molecular packing from the viewpoint of the possibility of performing solid-phase [2+2] photocycloaddition. The structures of different geometrical isomers of the dye and its complex with the magnesium cation were studied by quantum-chemical methods. Reversible geometrical photoisomerization of the dye and its complex with Mg^{2+} in acetonitrile solution was studied by spectrophotometry and ^1H NMR spectroscopy. It was demonstrated that photoirradiation of the complex of the *E*,*E* isomer with the magnesium cation leads predominantly to isomerization of the C=C double bond adjacent to the benzothiazolium fragment. Regioselective *E*,*E*→*Z*,*E* photoisomerization occurs *via* a singlet mechanism with a quantum yield of 0.45. The quantum yield of reverse *Z*,*E*→*E*,*E* photoisomerization is 0.52.

Experimental

The synthesis of dye **1b** has been described earlier.[8] Magnesium perchlorate (Aldrich) was dehydrated *in vacuo* at 240 °C. Acetonitrile (for HPLC) was additionally dehydrated by distillation over CaH_2. The percentage of water in acetonitrile-d_3 (Merck) was less than 0.05%.

X-ray diffraction study. Crystals of dye **1b** were grown by slow saturation of an acetonitrile solution of the dye with benzene vapor at ~20 °C. A single crystal was coated with a perfluorinated oil and mounted on a Bruker SMART-CCD diffractometer under a stream of cooled nitrogen. The experimental X-ray intensity data were collected from a single crystal (Mo-Kα radiation) using ω-scanning technique. The crystallographic parameters and characteristics of X-ray diffraction study are given in Table 5. The X-ray intensity data were processed using the Bruker SAINT software.[17] The structure was solved by direct methods and refined anisotropically by the full-matrix least-squares method against F^2. The hydrogen atoms were revealed from the difference Fourier synthesis and refined isotropically. All calculations were carried out using the SHELXTL-Plus program package.[18] The atomic coordinates and other experimental data were deposited with the Cambridge Structural Database* (CSD refcode 227165) and can be obtained from the authors.

Spectrophotometric studies. The absorption spectra were measured on a Specord-M40 spectrophotometer. All operations with solutions were carried out in a room illuminated by a red light. In studies of photoisomerization, acetonitrile solutions of the dye or its complex with the magnesium cation were placed in sealed quartz cells (1 cm) and irradiated using a DRSh-250 mercury lamp. The solutions contained atmospheric oxygen. Individual lines of the spectrum of the mercury lamp were separated using glass ligh filters. The intensity of actinic light was measured using a PP-1 cavity receiver. The overall error of measurement of the quantum yields of photoisomerization was ~20%.

The absorption spectrum of [(*Z*,*E*)-**1b**]·Mg^{2+} was calculated from the spectra of different photostationary states, which were established upon irradiation of the complex at a wavelength of 313, 365, 405, or 436 nm. Calculations were performed using self-modeling of the spectral matrix **D**, whose first column included the spectrum of [(*E*,*E*)-**1b**]·Mg^{2+}, and the next four columns included the spectra of different photostationary states. The spectra were measured in a range of 45000—19000 cm^{-1} with a step of 80 cm^{-1}.

In the calculation, the following two assumptions were used: 1) the photostationary mixture contains only one of three possible *Z* photoisomers, 2) the ratio of the quantum yields of the

* CCDC, 12 Union Road, Cambridge CB21EZ, UK (Fax: (+44)1223-336-033; E-mail: deposit@ccdc.cam.ac).

Table 5. Crystallographic characteristics of dye **1b** and details of X-ray diffraction study

Parameter	Characteristic
Molecular formula	$C_{33}H_{38}ClNO_9S$
Molecular weight, g mol^{-1}	660.15
Crystal system	Triclinic
Space group	$P\bar{1}$
a/Å	8.4700(2)
b/Å	10.6404(2)
c/Å	18.8191(5)
α/deg	78.967(1)
β/deg	86.544(1)
γ/deg	76.110(1)
V/Å^3	1615.85(6)
Z	2
ρ_{calc}/g cm^{-3}	1.357
F(000)	696
μ(Mo-$K\alpha$), mm^{-1}	0.238
Crystal dimensions/mm	0.32×0.28×0.18
T/K	120.0(2)
Radiation/Å	Mo-Kα (0.71073)
θ Scan mode/range/deg	ω/2.10—29.00
Ranges of indices of measured reflections	$-11 \le h \le 11$, $-14 \le k \le 14$, $-25 \le l \le 14$
Number of measured reflections	10653
Number of independent reflections	7706 (R(int) = 0.0206)
Number of reflections with $I > 2\sigma(I)$	6150
Number of refinement parameters	559
R factors based on all reflections with $I > 2\sigma(I)$	$R_1 = 0.0419$, $wR_2 = 0.1000$ $R_1 = 0.0579$, $wR_2 = 0.1060$
Goodness-of-fit on F^2	1.023
Residual electron density, min/max, e/Å^3	−0.369/0.720

forward and reverse photoisomerization (Q_{E-Z}) is independent of the wavelength of irradiation. The value of Q_{E-Z} was postulated and then the fractional concentrations of the E,E and Z,E isomers in different photostationary states were calculated from the changes in the optical density of the solution at the irradiation wavelength. Then the matrix of the fractional concentrations **C** was composed. The first row of this matrix included the fractional concentrations of the E,E isomer, and the second row included the corresponding values for the Z,E isomer. The data matrix **D** is related to the matrix **C** by the equation **D** = **EC**, where **E** is a two-column matrix containing the spectra of the E,E and Z,E isomers. The theoretical spectral matrix for these isomers was calculated by the equation $\mathbf{E}' = \mathbf{DC}^T(\mathbf{CC}^T)^{-1}$, where $\mathbf{C}^T$ is the transposed matrix **C**. Then the theoretical spectral matrix was calculated by the equation $\mathbf{D}' = \mathbf{E}'\mathbf{C}$. The minimum standard deviation between the experimental matrix **D** and the reconstructed matrix **D**′ was determined by varying Q_{E-Z}. The standard deviation thus determined was no higher than 0.001 (in optical density units), which counts in favor of the above-mentioned assumptions. The output data of this calculation included Q_{E-Z}, the spectrum of $[(Z,E)$-**1b**$] \cdot Mg^{2+}$, and the fractional concentrations of the isomers in four photostationary states.

The quantum yield of the forward isomerization was determined from the dependence of the fractional concentration of $[(E,E)$-**1b**$] \cdot Mg^{2+}$ on the time of irradiation at λ = 365 nm. The fractional concentrations were evaluated from the absorption spectra using the calculated spectrum of $[(Z,E)$-**1b**$] \cdot Mg^{2+}$. The quantum yield was estimated by minimization of the standard deviation between the experimental and theoretical fractional concentrations of $[(E,E)$-**1b**$] \cdot Mg^{2+}$. The latter were calculated by solving the differential equation for the reversible first-order reaction.

A sample of a photostationary mixture of the isomers for NMR studies was prepared by irradiation of a solution of $[(E,E)$-**1b**$] \cdot Mg^{2+}$ ($1.5 \cdot 10^{-4}$ mol L^{-1}, ~15 mL) at a wavelength of 365 nm. The solution was placed in a special quartz cell with an optical path length of about 1 mm and the irradiated surface area of 150 cm^2. After establishment of a photostationary state (spectrophotometric control), the solution was poured into a sealed flask and concentrated to dryness at low temperature using a forepump.

The ^1H NMR spectra were measured on a Bruker DRX500 spectrometer (500.13 MHz) in CD_3CN at 25 °C using the solvent as the internal standard (δ 1.96). The signals were assigned based on the two-dimensional ^1H-^1H COSY and NOESY spectra. The chemical shifts and the spin-spin coupling constants were measured with an accuracy of 0.01 ppm and 0.1 Hz, respectively.

Quantum-chemical calculations. The equilibrium geometry and harmonic vibrational frequencies were calculated by the DFT method using the quantum-chemical program written by Laikov.[19] Calculations were performed with the employment of the generalized gradient approximation[20] and triple zeta Gaussian basis set[21] for all atoms optimized for calculations by the DFT method using the expansion of the electron density in an auxiliary basis set. This approximate approach allows one to substantially accelerate calculations of the Coulomb and exchange correlation contributions. The chosen density functional is characterized by the absence of empirical parameters and adequately reproduces many molecular properties, such as the equilibrium geometry, bond energies, and vibrational frequencies.[22] Calculations by the PM3 method[23] were carried out with the use of a standard parameter set.

This study was financially supported by the Russian Foundation for Basic Research (RFBR, Project Nos. 01-03-32474, 02-03-32286, 03-03-32178, and 03-03-32929), the German Research Foundation (DFG, Deutsche Forschungsgemeinschaft; RFBR-DFG Grant No. 02-03-04003), the Foundation of the President of the Russian Federation (Grant MK-3666.2004.3), the INTAS (Grant 2001-0267), the Ministry of Science and Technology of the Russian Federation, and the Russian Academy of Sciences.

References

1. T. I. Sergeeva, S. Yu. Zaitsev, M. S. Tsarkova, S. P. Gromov, A. I. Vedernikov, M. S. Kapichnikova, M. V. Alfimov, T. S. Druzhinina, and D. Möbius, *J. Colloid Interface Science*, 2003, **265**, 77.

2. M. V. Alfimov and S. P. Gromov, in *Applied Fluorescence in Chemistry, Biology, and Medicine*, Eds W. Rettig, B. Strehmel, S. Schrader, and H. Seifert, Springer-Verlag, Berlin, 1999, 161.
3. M. V. Alfimov, O. A. Fedorova, and S. P. Gromov, *J. Photochem. Photobiol., A*, 2003, **158**, 183.
4. S. P. Gromov and M. V. Alfimov, *Izv. Akad. Nauk, Ser. Khim.*, 1997, 641 [*Russ. Chem. Bull.*, 1997, **46**, 611 (Engl. Transl.)].
5. S. P. Gromov, *Ros. Khim. Zh.*, 2001, **45**, 116 [*Mendeleev Chem. J.*, 2001, **45** (Engl. Transl.)].
6. S. P. Gromov, S. A. Sergeev, S. I. Druzhinin, M. V. Rusalov, B. M. Uzhinov, L. G. Kuz´mina, A. V. Churakov, J. A. K. Howard, and M. V. Alfimov, *Izv. Akad. Nauk, Ser. Khim.*, 1999, 530 [*Russ. Chem. Bull.*, 1999, **48**, 525 (Engl. Transl.)].
7. S. I. Druzhinin, M. V. Rusalov, B. M. Uzhinov, S. P. Gromov, S. A. Sergeev, and M. V. Alfimov, *J. Fluor.*, 1999, **9**, 33.
8. S. P. Gromov, A. I. Vedernikov, E. N. Ushakov, L. G. Kuz´mina, A. V. Feofanov, V. G. Avakyan, A. V. Churakov, Yu. S. Alaverdyan, E. V. Malysheva, M. V. Alfimov, J. A. K. Howard, B. Eliasson, and U. G. Edlund, *Helv. Chim. Acta*, 2002, **85**, 60.
9. M. V. Alfimov, S. P. Gromov, Yu. V. Fedorov, O. A. Fedorova, A. I. Vedernikov, A. V. Churakov, L. G. Kuz´mina, J. A. K. Howard, S. Bossmann, A. Braun, M. Woerner, D. F. Sears, and J. Saltiel, *J. Am. Chem. Soc.*, 1999, **121**, 4992.
10. O. A. Fedorova, Yu. V. Fedorov, A. I. Vedernikov, O. V. Yescheulova, S. P. Gromov, M. V. Alfimov, L. G. Kuz´mina, A. V. Churakov, J. A. K. Howard, S. Yu. Zaitsev, T. I. Sergeeva, and D. Mцbius, *New J. Chem.*, 2002, **26**, 543.
11. Yu. V. Fedorov, O. A. Fedorova, E. N. Andryukhina, S. P. Gromov, M. V. Alfimov, L. G. Kuz´mina, A. V. Churakov, J. A. K. Howard, and J.-J. Aaron, *New J. Chem.*, 2003, **27**, 280.
12. L. G. Kuz´mina, A. V. Churakov, J. A. K. Howard, O. A. Fedorova, S. P. Gromov, and M. V. Alfimov, *Kristallografiya*, 2003, **48**, 664 [*Crystallogr. Repts.*, 2003, **48**, 613 (Engl. Transl.)].
13. S. P. Gromov, S. N. Dmitrieva, A. I. Vedernikov, L. G. Kuz´mina, A. V. Churakov, Yu. A. Strelenko, and J. A. K. Howard, *Eur. J. Org. Chem.*, 2003, 3189.
14. F. H. Allen, O. Kennard, D. G. Watson, L. Brammer, A. G. Orpen, and R. Taylor, *J. Chem. Soc., Perkin Trans. 2*, 1987, S1.
15. H. Braatz, S. Hecht, H. Seifert, S. Helm, J. Bendig, and W. Rettig, *J. Photochem. Photobiol. A: Chem.*, 1999, **123**, 99.
16. J. Liu, E. L. Suits, and K. J. Boarman, *Tetrahedron Lett.*, 2003, **44**, 8103.
17. SAINT, Version 6.02A, Bruker AXS Inc., Madison, Wisconsin (USA), 2001.
18. SHELXTL-Plus, Release 5.10, Bruker AXS Inc., Madison, Wisconsin (USA), 1997.
19. D. N. Laikov, *Chem. Phys. Lett.*, 1997, **281**, 151.
20. J. P. Perdew, K. Burke, and M. Ernzerhof, *Phys. Rev. Lett.*, 1996, **77**, 3865.
21. D. N. Laikov, Ph. D. (Phys.-Mat.) Thesis, M. V. Lomonosov Moscow State University, Moscow, 2000 (in Russian).
22. C. Adamo and V. Barone, *J. Chem. Phys.*, 1999, **110**, 6158.
23. J. J. P. Stewart, *J. Comput. Chem.*, 1989, **10**, 209.

Received December 24, 2003